

Neutron scattering and *ab initio* molecular-dynamics study of vibrations in glassy GeSe₂

R. L. Cappelletti, Mark Cobb, and D. A. Drabold

Department of Physics and Astronomy, Condensed Matter and Surface Science Program, Ohio University, Athens, Ohio 45701-2979

W. A. Kamitakahara

Reactor Radiation Division, National Institute of Standards and Technology, Gaithersburg, Maryland 20899

(Received 15 February 1995; revised manuscript received 27 April 1995)

The dynamics of glassy GeSe₂ have been investigated through a combined experimental and theoretical approach. Particular attention was devoted to vibrational modes with energies around 25 meV (200 cm⁻¹), with regard to the interpretation of features (*A*₁ and *A*_{1c}) observed by Raman spectroscopy. *Ab initio* local-density-functional molecular-dynamics calculations have been carried out for a 63-atom model with periodic boundary conditions. The results are in good agreement with time-of-flight inelastic-neutron-scattering measurements of the vibrational density of states and of the dynamic structure factor of GeSe₂. The motions associated with the *A*_{1c} band are shown to be dominated by breathing motions of edge-sharing Se₄ tetrahedra around Ge atoms. There is also a substantial contribution from modes localized on network defects.

The value of neutron-scattering experiments on the structure and dynamics of glasses is greatly enhanced when the results can be interpreted in terms of realistic computer simulations. In the following, we show that *ab initio* molecular-dynamics simulations provide another very valuable tool in the interpretation of neutron data. Using relatively small cells, this method appears to be particularly powerful for compound network glasses such as the chalcogenides. By means of such calculations disordered model structures can be generated which result from electronic and ionic interactions at the most basic level. Applying this approach to a 63-atom model of glassy GeSe₂, we have been able to identify in detail the atomic motions associated with the *A*₁ and *A*_{1c} modes observed in Raman scattering experiments^{1,2} and in this work. The structure of this glass remains controversial,^{2,3} and the interpretation of the *A*_{1c} mode and of the first sharp diffraction peak in the static structure factor are relevant issues. Within the limitations imposed by its size, the model provides an excellent description of the static structure factor, vibrational density of states (VDOS), and wave vector (*Q*) dependence of the inelastically scattered neutron intensity *S*(*Q*, *E*).

A new set of neutron-scattering data was required to furnish a good basis for comparison with the model. These results were obtained on a 42 g portion of the same, carefully prepared, GeSe₂ sample used in the extensive neutron scattering study of Walter *et al.*⁴ The current experiment was designed to provide sufficient energy resolution in the energy region around 25 meV to distinguish between *A*₁ and *A*_{1c} modes, while at the same time providing enough *Q* range to compare with calculations of *S*(*Q*, *E*). The data were obtained on the Fermi-Chopper time-of-flight spectrometer at the Cold Neutron

Research Facility of the National Institute of Standards and Technology. An incident neutron energy of 14 meV was employed, and the vibrational spectrum was measured in neutron energy gain, with the sample at room temperature. Standard procedures were employed to obtain the vibrational density of states (Fig. 1) corrected for multiphonon effects.

The neutron time-of-flight measurements were treated as follows. After subtracting the smoothed results of an empty aluminum foil container run and correcting detector efficiencies using the results of a separate vanadium sample run, the data were reduced to provide a neutron

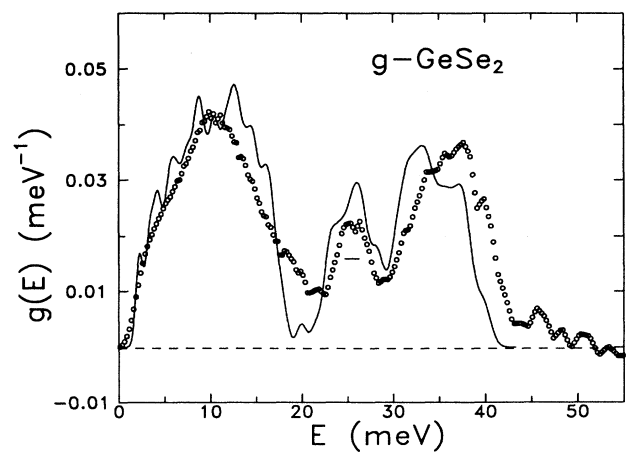


FIG. 1. Vibrational density of states of *g*-GeSe₂: solid curve, theory; open circles, experiment. The short line under the central peak shows the FWHM of the time-of-flight spectrometer in this energy range.

VDOS with corrections for multiphonon scattering as described previously.⁵ Other corrections are not expected to alter the shape of the VDOS reported here. Indeed, where they can be compared the results are in very good agreement with the previous measurements of Walter *et al.*⁴ on the same sample. Our dynamical structure factors are not normalized as were theirs, but the shapes are in good agreement. Since the work of Walter *et al.* was completed several years ago, we checked the sample for evidence of reversion to the crystalline state by determining $S(Q,0)$ from the time-of-flight measurements between $Q = 1.5$ and 5 \AA^{-1} and also from measurements made with the triple-axis spectrometer BT-4 at NIST between $Q=0.5$ and 3.5 \AA^{-1} . The results are in excellent agreement with Ref. 4.

Computations described here used the *ab initio*, local basis density-functional method of Sankey and co-workers.⁶ The essential approximations are (1) Bachelet-Hamann-Schlüter pseudopotentials, (2) the Harris functional, (3) the local-density approximation, (4) a minimal basis set of one *s* and three *p* confined pseudoatomic orbitals per site. The method has met with great success in a wide variety of systems, and provides a transferable description of covalently bonded materials.

Two models were constructed with 62- or 63-atom simple cubic supercells. The calculations were carried out at constant volume and used a time step of 2.5 fs. In quenching, four special *k* points were used for sampling the small Brillouin zone to compute energies and forces. For annealing studies the Γ ($\vec{k} = \vec{0}$) point was used. A first crude model was formed by placing 20 Ge and 43 Se randomly on sites of a diamond lattice. Then the cell was (1) annealed at 5000 K for 1 ps,⁷ (2) equilibrated at 1500 K, (3) cooled over 4 ps to $T=300$ K, (4) quenched to $T=0$ K. The bonding was quite reasonable, with the exception of a Se trimer, which was modified by removing the middle Se and annealing and quenching the resulting 62-atom cell. The cell has a pair distribution function, static structure factor, dynamic structure factor, and a vibrational spectrum in impressive agreement with experiment, considering the small cell size and the *ad hoc* procedure used to form the structure (see below). In order to test the robustness of the procedure, and to get the exact stoichiometry for GeSe_2 , we added a Ge atom and annealed the cell at 1500 K for 6 ps. The cell was then cooled to 300 K over 4.2 ps, and then quenched to $T=0$. This cell has a density suited to *g*- GeSe_2 : 4.2 gm/cc. The anneal at 1500 K led to substantial diffusion, and a well equilibrated liquid. The second cell's structural and dynamical properties were quite similar to the first. In the rest of the paper our discussion is based on the second model.

The dynamical matrix is determined by displacing each atom by 0.03 \AA in each of three orthogonal directions and performing *ab initio* force calculations for all the atoms for each such displacement. Each such calculation yields a column of the force constant matrix.⁸ The vibrational eigenvectors and eigenvalues of the supercell are then easily obtained. The VDOS calculated for comparison with experiment was obtained by summing Gaussians centered at each eigenvalue having FWHM corresponding to the

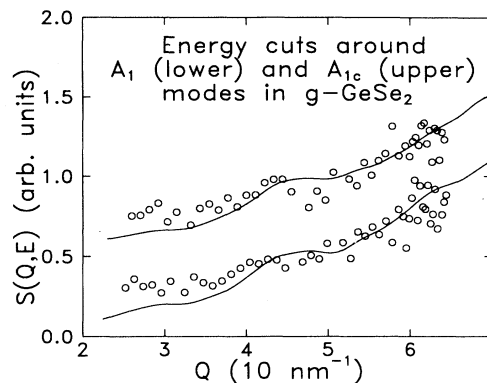


FIG. 2. Dynamical structure factors: experiment, open circles; theory, solid line. The upper set has been vertically shifted up by 0.5 units for clarity. See text for details on energy cut.

experimental resolution. The results are shown as the solid line in Fig. 1 where we see that the principal features of the spectrum are reproduced.

The A_1 and A_{1c} modes are contained in the measured feature in Fig. 1 centered about 25 meV. While no definite minimum between the two peaks is observed, the energy resolution (FWHM 1.6 meV in this energy range) was good enough to allow the Q dependence of the scattering of the A_1 region (22.5 to 26.5 meV) to be traced without much interference with the A_{1c} region (26.5 to 28.5 meV), with the results plotted in Fig. 2. The Q dependences are very similar, implying that the dynamic correlations associated with A_1 and A_{1c} are quite similar. It is probable that the 25 meV feature in this glass would appear with much the same shape as in Fig. 1 in any neutron-scattering experiment, even if much better energy resolution were available. Sugai¹ gives a Raman FWHM of 2.13 meV for the A_1 and a FWHM of 1.23 meV for the A_{1c} . Because transition-probability weighting selects modes in Raman scattering and does not in neutron scattering, the measured neutron widths are expected to be larger since other modes are mixed in.

Using the above molecular-dynamics (MD) simulation, the theoretical dynamical structure factors were computed from Eq. (8) of Walter *et al.*⁴ with broadening chosen to be suitable to the experimental resolution and statistics. The resulting structure factors agree rather well with the experiment (see Fig. 2).

The computed normal modes can be animated by creating a set of files of atomic displacements along each eigenvector which vary sinusoidally in time and displaying them in sequence on a computer screen using the program "XMol."⁹ In this manner we have visually examined each mode and focused on those specific to the A_1 and A_{1c} segments of the spectrum.

While the motion in each band is complicated, certain simple features appear. In particular, we find that the A_1 band is dominated by modes more or less extended throughout the supercell which are largely breathing motions of tetrahedra, i.e., the eigenvectors of the Se atoms surrounding a Ge atom in a tetrahedron lie mainly along

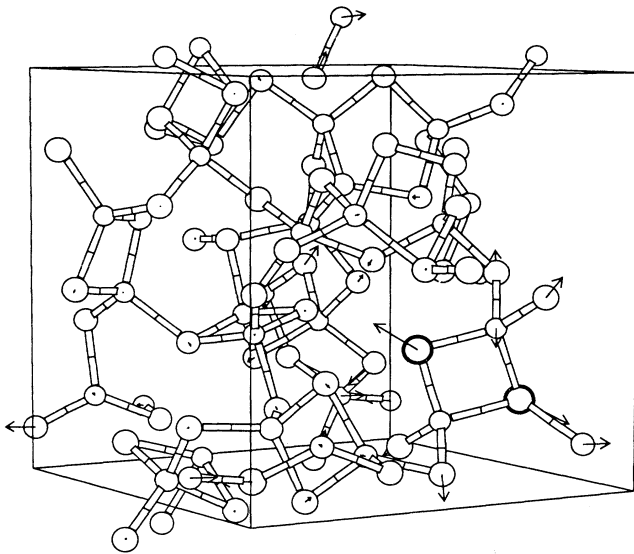


FIG. 3. A view of the atomic motions of a mode in the A_{1c} region of the spectrum. Arrows on each atom represent calculated eigenvalues. Two edge-sharing tetrahedra, marked by two dark-circled Se atoms, show a partially localized bite-tetrahedral breathing mode.

the lines joining them to the Ge atom. One sees this motion somewhat localized on particular tetrahedra in the cell, and on different tetrahedra in neighboring modes within the band. There are also more localized tetrahedral breathing modes. Most of the tetrahedra in the supercell share one or more of their corners with another tetrahedron. In addition, we find motions of edge-sharing tetrahedra in this region. About 1/4 of all Se atoms in the cell are found along edges shared by two tetrahedra. In particular, we noticed a localized motion in which the outer four Se atoms of a bitetrahedron "rock" symmetrically while the Ge and shared Se atoms are nearly at rest.

The calculated modes in the A_{1c} band can likewise be described in two categories: first, there are partially localized breathing motions of the edge-sharing tetrahedra accounting for about 2/3 of the modes in this region. Among these are modes nearly identical to those described by Sugai.¹ An example is shown in Fig. 3 (which was generated by "XMol"). Second, about 1/3 of the modes in the models are more localized and associated with network defects. A conventional measure of mode localization is the inverse participation ratio (IPR) which is large for localized modes.¹⁰ The IPR for the 63-atom model glass is shown in Fig. 4(a) where a sharp onset of localization is seen near mode index 100. In Fig. 4(b) the IPR's for the A_1 and A_{1c} bands are compared, the latter showing considerably more localization.

Several types of network defects appear in the model glass, and two of these contribute significantly in the A_{1c} band: triply coordinated Se and singly coordinated Se. The defects are found by measuring bond lengths between atoms in the model and comparing them to expected values for Se-Ge or Se-Se. In particular, there

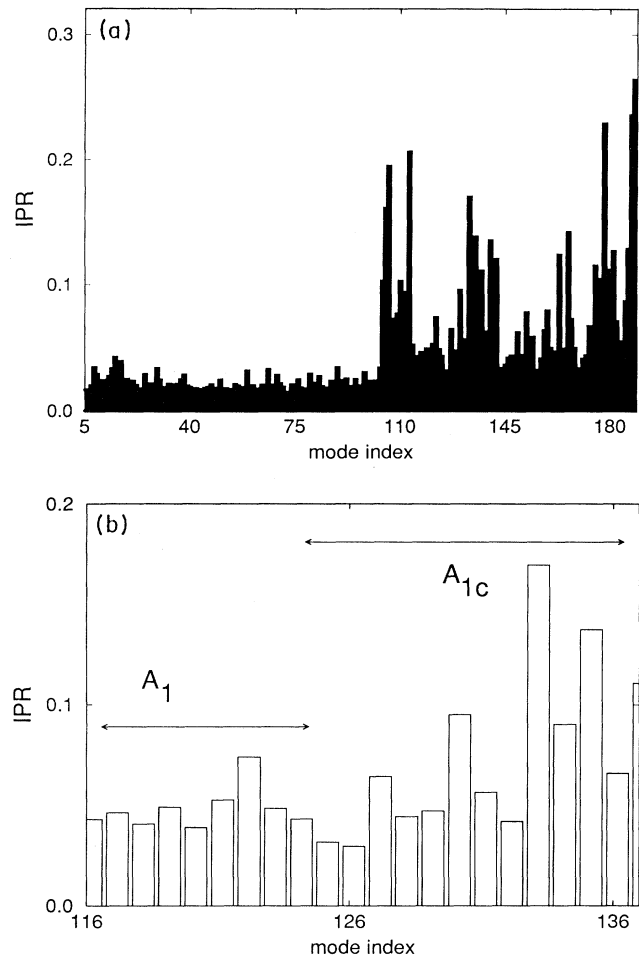


FIG. 4. Inverse participation ratios (IPR) for the 63-atom model; (a) IPR for entire vibrational eigenvalue spectrum, (b) blowup of the A_1 and A_{1c} energy range. For reference, the calculated A_1 band involves modes 116–124 (corresponding to 24.4–26.2 meV), and the A_{1c} involves modes 124–137 (mode 137 has an energy of 30.0 meV).

are several examples of a motion strongly localized on tetrahedra containing a singly coordinated Se. This type of defect appears to be associated with another, namely triply coordinated Ge, which occurs with roughly the same statistics. Localized modes associated with this latter defect are found at 20 meV, close to the small peak between the first broadband in the measured VDOS and the smaller central band containing the A_1 and A_{1c} bands.

The static structure factor of the 63-atom model is shown as the upper line in Fig. 5, and is in reasonable agreement with the experimental measurements taken from Fig. 5 of Ref. 4 (lower curve and points). In particular, the location of all the principal peaks are close to the measured ones. A noticeable discrepancy is the small feature at 2.50 \AA^{-1} . Because of finite size effects (the artificial periodicity associated with the supercell), we show calculated $S(Q)$ for $Q > 1 \text{ \AA}^{-1}$.

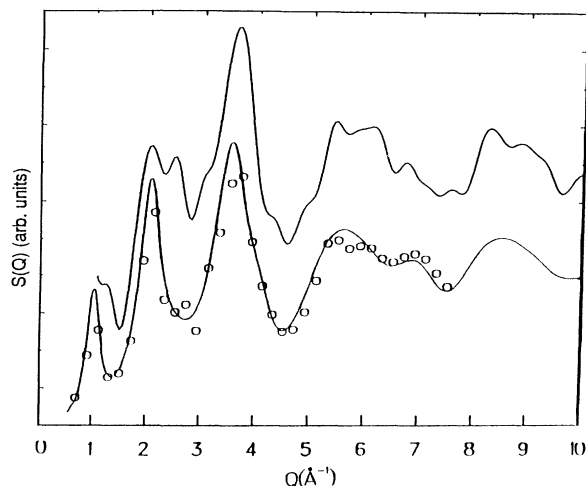


FIG. 5. Upper curve, static structure factor for 63-atom model. Only $Q > 1.0 \text{ \AA}^{-1}$ is shown because of periodic boundary condition artifacts. The lower curve and points are experimental results from Fig. 5 of Ref. 4.

To check on the above results we have begun a study extending the calculations to a 216-atom cell. Calculations of vibrational properties are still in progress, but the structural results are in very good agreement with the measured $S(Q)$, the anomaly at 2.50 \AA^{-1} nearly disappearing. It is also gratifying that the simulation is accurate in the placement and weight of the first sharp diffraction peak, often taken to be a signature of the intermediate range order (IRO). We expect further study of this model to elucidate the origin of this peak. Moreover, these studies support the smaller cell study in terms of the statistics of corner and edge-sharing tetrahedra. In addition, they show that about 25% of the Ge participate

in Ge-Ge "wrong" bonds within the structure. Of these 14% are in ethanelike configurations and the remaining 11% are in other configurations (defects of various kinds.) Mössbauer measurements using a small amount of Sn as a probe of the Ge sites^{11,12} show two peaks the larger of which has been identified with Ge in tetrahedral sites accounting for 85% of the Ge and the smaller with ethanelike sites accounting for 15% of the Ge. It appears that the model contains more defects than the real glass, which is not unexpected.

Vashishta and co-workers¹³ performed MD simulations with empirical potentials on a 648-atom cell of GeSe₂ and obtained $S(Q)$ in semiquantitative agreement with experiment and a VDOS which agreed less well. The present *ab initio* calculation on a 63-atom cell yields a significantly improved VDOS. Our preliminary $S(Q)$ results on the 216-atom model are comparable in agreement with experiment to Ref. 13 but give a more accurate placement of the first sharp diffraction peak.

In summary, the *ab initio* MD calculations on a 63-atom model of *g*-GeSe₂ described here are in excellent agreement with neutron-scattering measurements presented in this work. These calculations provide detailed insights into the dynamics of *g*-GeSe₂ in the regions of the A_1 and A_{1c} bands. A more complete MD study is underway on a 216-atom model. We expect to report on structural information and elucidate its connection to the various portions of the measured vibrational spectrum, describe the atomistics of the IRO, and give an account of light-induced metastability.¹⁴

We are grateful to David L. Price of Argonne National Laboratory for providing us the sample for use in this experiment. This work was partially completed while R.L.C. was on contract with NIST. D.A.D. acknowledges partial support from NSF Grant No. DMR 93-22412 and from the Ohio Supercomputer Center under Grant No. PHS218-1.

¹ S. Sugai, Phys. Rev. B **35**, 1345 (1987).

² R. J. Nemanich *et al.*, Physica B+C **117-118B**, 959 (1983).

³ P. M. Bridenbaugh, G. P. Espinosa, J. E. Griffiths, J. C. Phillips, and J. P. Remeika, Phys. Rev. B **20**, 4140 (1979); J. C. Phillips, J. Non-Cryst. Solids **43**, 37 (1981); J. E. Griffiths *et al.*, Phys. Status Solidi B **122**, K11 (1984).

⁴ U. Walter, D. L. Price, S. Susman, and K. J. Volin, Phys. Rev. B **37**, 4232 (1988).

⁵ W. A. Kamitakahara, R. L. Cappelletti, P. Boolchand, B. Halfpap, F. Gompf, D. A. Neumann, and H. Mutka, Phys. Rev. B **44**, 94 (1991).

⁶ Otto F. Sankey and D. J. Niklewski, Phys. Rev. B **40**, 3979 (1989); Otto F. Sankey, D. A. Drabold, and G. B. Adams, Bull. Am. Phys. Soc. **36**, 924 (1991).

⁷ Annealing and slow quenching employed Berendsen thermostat, H. J. C. Berendsen *et al.*, J. Chem. Phys. **81**, 3684

(1984).

⁸ O. F. Sankey (unpublished).

⁹ XMol, version 1.3.1, Minnesota Supercomputer Center, Inc., Minneapolis, MN, 1993.

¹⁰ See, for example, S. R. Elliot, *Physics of Amorphous Materials*, by 2nd ed. (Longman Group, UK Limited, 1990), p. 201.

¹¹ M. Stevens, P. Boolchand, and J. G. Hernandez, Phys. Rev. B **31**, 981 (1985).

¹² M. J. Peters and L. E. McNeil, J. Non-Cryst. Solids **139**, 231 (1992).

¹³ P. Vashishta, Rajiv K. Kalia, and I. Ebbsjö, Phys. Rev. B **39**, 6034 (1989).

¹⁴ M. Cobb, D. A. Drabold, and R. L. Cappelletti (unpublished).